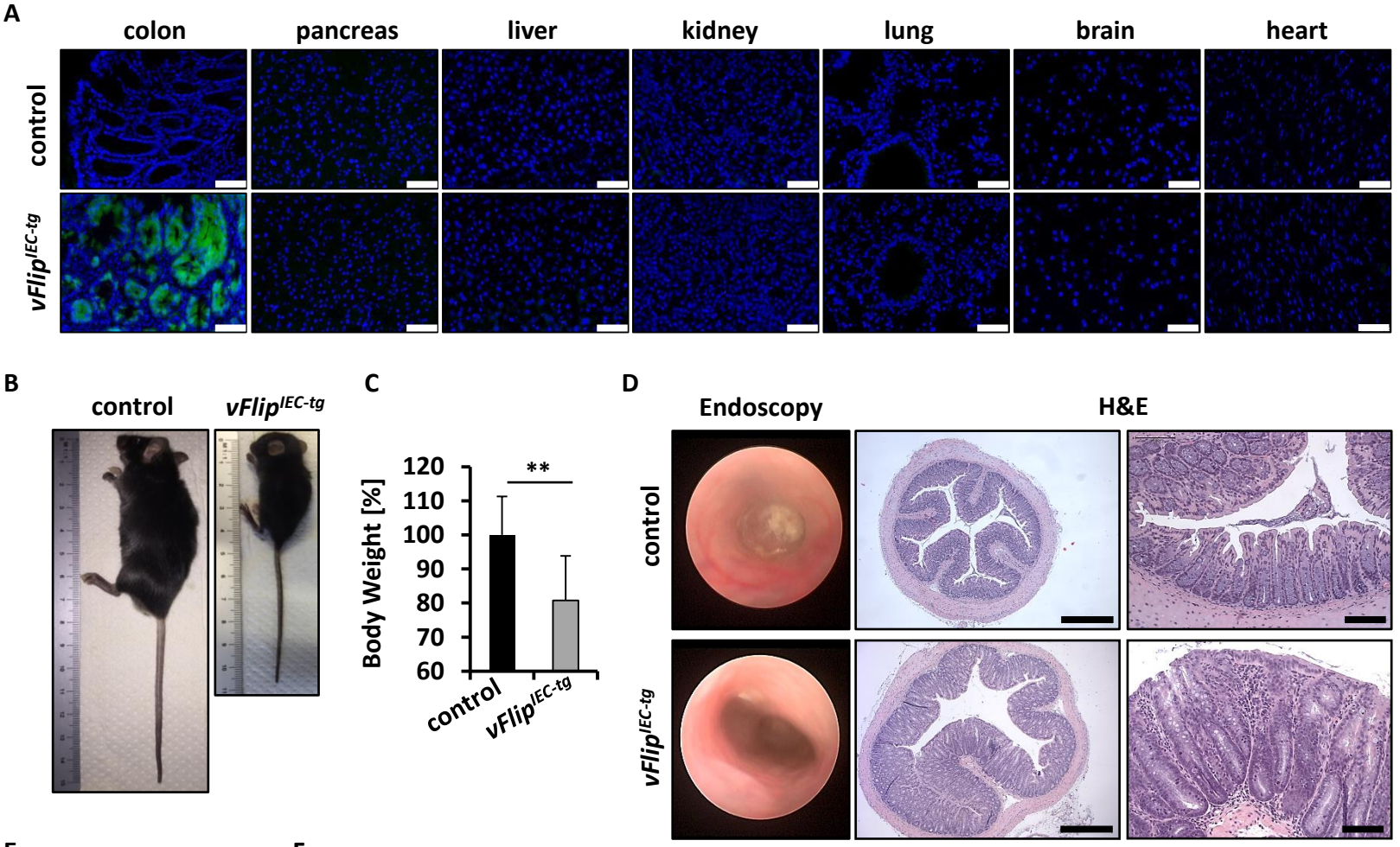
A
colon
pancreas
liver
kidney
lung
brain
heart
control
vFlip IEC-tg
B
control
vFlip IEC-tg
C
Body Weight [%]
120
110
100
90
80
70
60
**
control
vFlip IEC-tg
D
Endoscopy
H&E
control
vFlip IEC-tg
E
Histology Score
4
3
2
1
0
***
control
vFlip IEC-tg
F
Gene Expression [fold change]
30
20
10
0
***
**
Tnfa
S100a9
control
vFlip IEC-tg

Suppl. Fig. 1

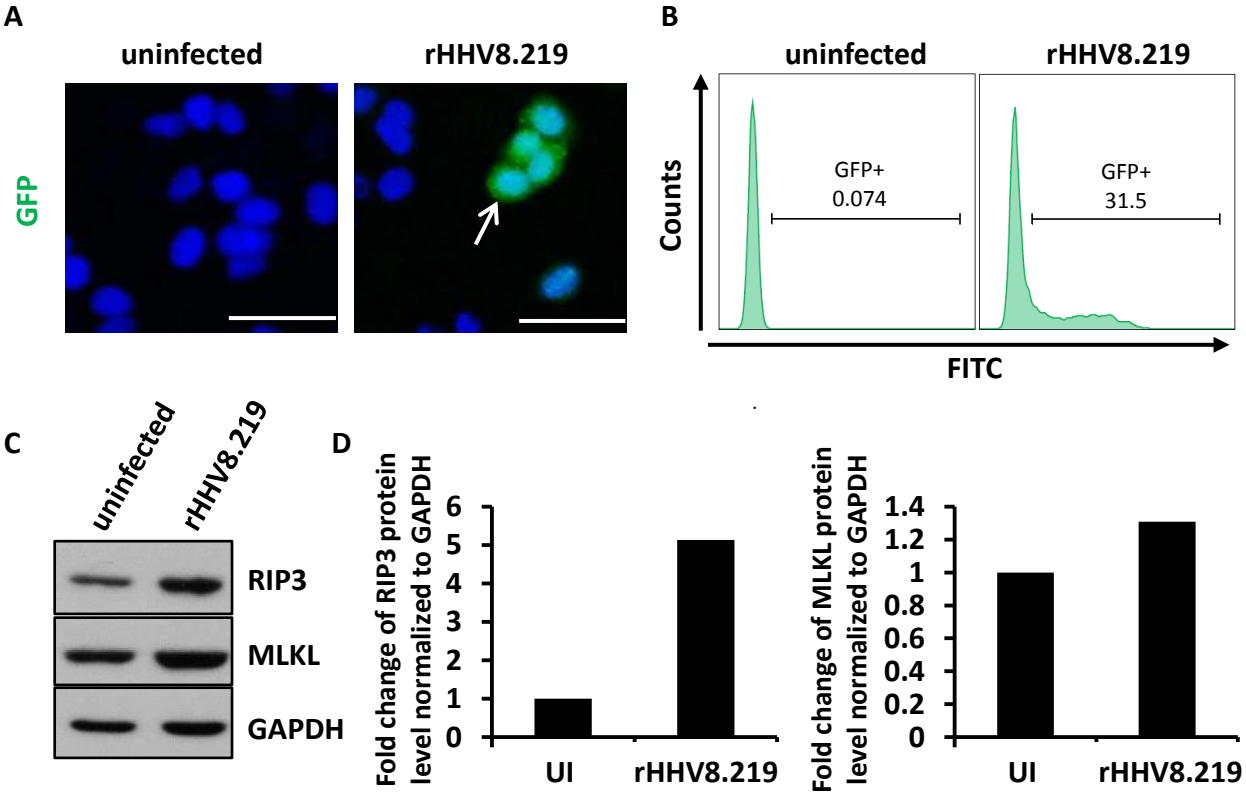
A
uninfected
rHHV8.219
GFP
B
uninfected
rHHV8.219
Counts
GFP+
0.074
GFP+
31.5
FITC
C
uninfected
rHHV8.219
RIP3
MLKL
GAPDH
D
Fold change of RIP3 protein level normalized to GAPDH
0
1
2
3
4
5
6
UI
rHHV8.219
Fold change of MLKL protein level normalized to GAPDH
0
0.2
0.4
0.6
0.8
1
1.2
1.4
UI
rHHV8.219

Suppl. Fig. 2

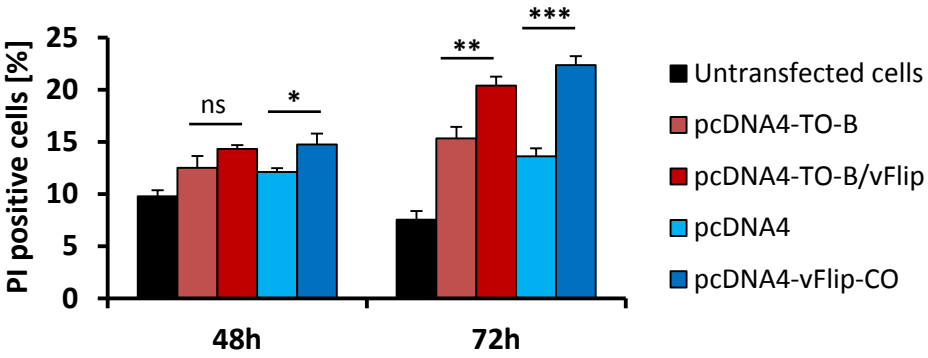
PI positive cells [%]
25
20
15
10
5
0
ns
*
**
***
48h
72h
Untransfected cells
pcDNA4-TO-B
pcDNA4-TO-B/vFlip
pcDNA4
pcDNA4-vFlip-CO

Suppl. Fig. 3

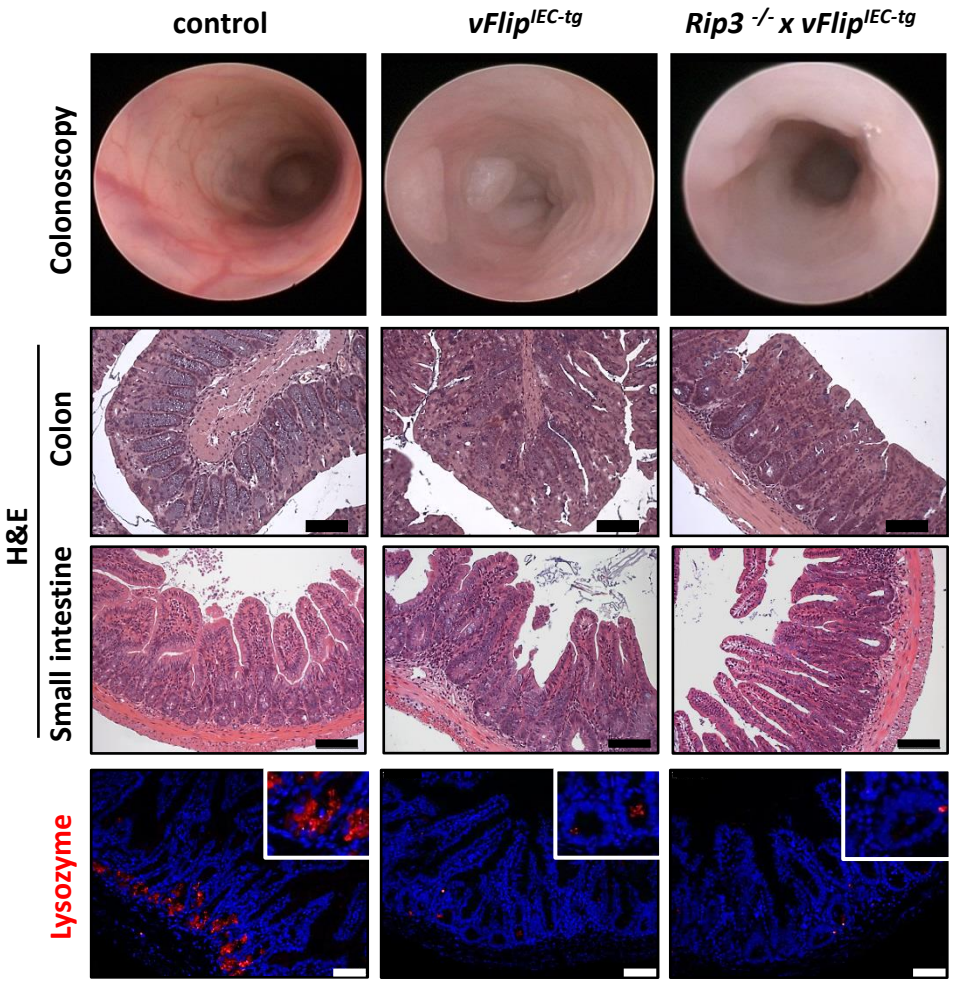
control
vFlip IEC-tg
Rip3 -/- x vFlip IEC-tg
Colonoscopy
H&E
Colon
Small intestine
Lysozyme

Suppl. Fig. 4

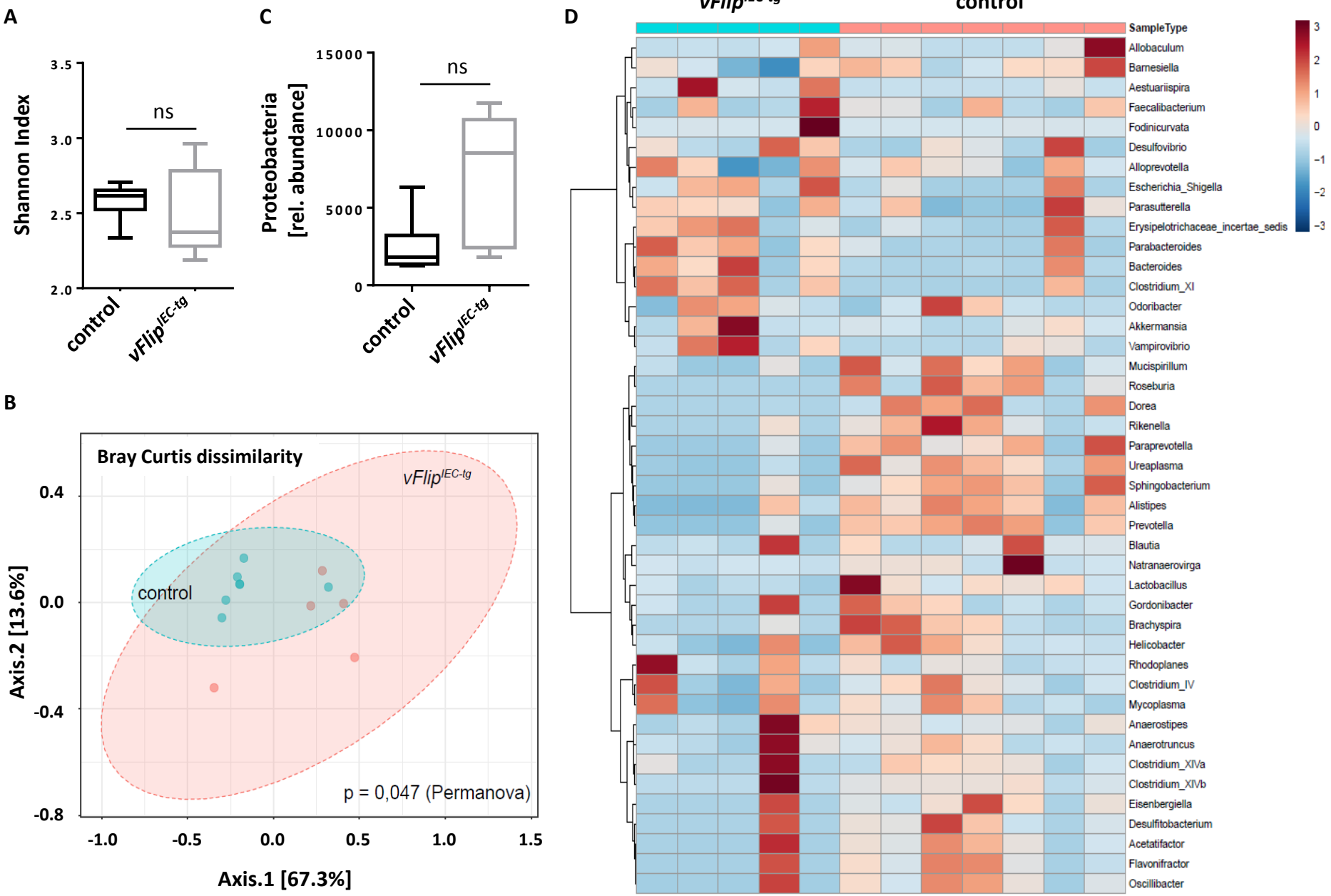
A
Shannon Index
3.5
3.0
2.5
2.0
ns
control
vFlip IEC-tg
C
Proteobacteria [rel. abundance]
15000
10000
5000
0
ns
control
vFlip IEC-tg
B
Bray Curtis dissimilarity
vFlip IEC-tg
control
p = 0,047 (Permanova)
Axis.2 [13.6%]
0.4
0.0
-0.4
-0.8
-1.0
-0.5
0.0
0.5
1.0
1.5
Axis.1 [67.3%]
D
vFlip IEC-tg
control
SampleType
Allobaculum
Barnesiella
Aestuariispira
Faecalibacterium
Fodinicurvata
Desulfovibrio
Alloprevotella
Escherichia_Shigella
Parasutterella
Erysipelotrichaceae_incertae_sedis
Parabacteroides
Bacteroides
Clostridium_XI
Odoribacter
Akkermansia
Vampirovibrio
Mucispirillum
Roseburia
Dorea
Rikenella
Paraprevotella
Ureaplasma
Sphingobacterium
Alistipes
Prevotella
Blautia
Natranaerovirga
Lactobacillus
Gordonibacter
Brachyspira
Helicobacter
Rhodoplanes
Clostridium_IV
Mycoplasma
Anaerostipes
Anaerotruncus
Clostridium_XIVa
Clostridium_XIVb
Eisenbergiella
Desulfitobacterium
Acetatifactor
Flavonifractor
Oscillibacter
3
2
1
0
-1
-2
-3

Suppl. Fig. 5

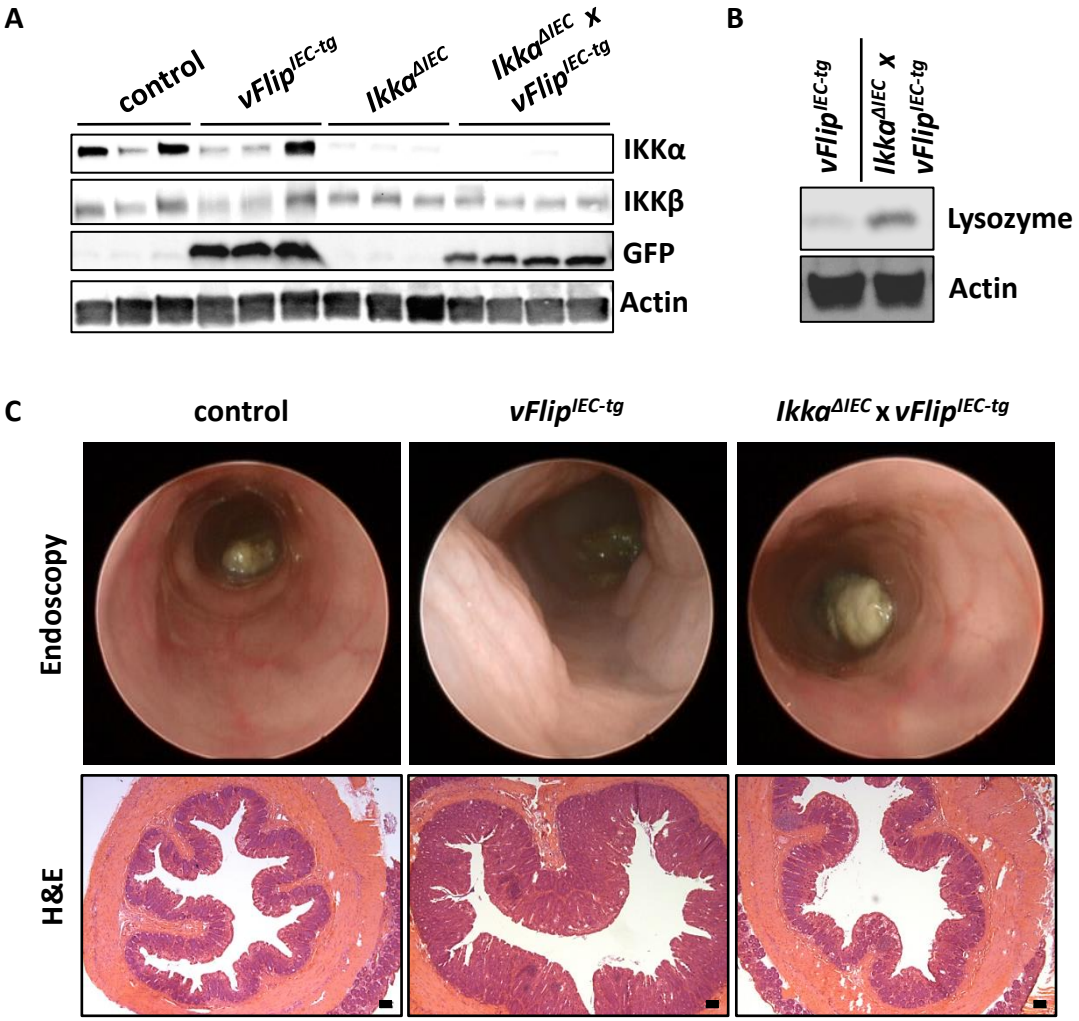
A
control
vFlip IEC-tg
Ikkα ΔIEC
Ikkα ΔIEC x vFlip IEC-tg
IKKα
IKKβ
GFP
Actin
B
vFlip IEC-tg
Ikkα ΔIEC x vFlip IEC-tg
Lysozyme
Actin
C
control
vFlip IEC-tg
Ikkα ΔIEC x vFlip IEC-tg
Endoscopy
H&E

Suppl. Fig. 6

Supplementary Information

Supplemental experimental procedures

Histology Scoring

Pathology scoring of the small intestine was performed on H&E stained small intestinal tissue sections by averaging the total amount of (a) Integrity of the intestinal epithelium: intact and no pathological changes (0), mild, moderate, severe destruction (1,2,3), (b) Mucosal inflammation: no inflammatory infiltrates (0), rare, moderate or massive invasion of immune cells (1,2,3) and (c) Paneth cells: no pathological changes (0), rare, moderate or massive loss of Paneth cells (1,2,3). For histology scoring of the small intestine whole cross sections of at least 10 individual animals per group were analyzed.

Pathology scoring of the colon was performed on H&E stained colon sections by averaging the total amount of (a) Integrity of the intestinal epithelium: intact and no pathological changes (0), mild, moderate, severe destruction (1,2,3) and (b) Mucosal inflammation: no inflammatory infiltrates (0), rare, moderate or massive invasion of immune cells (1,2,3). Whole cross sections of at least 16 individual animals per group were analyzed.

Quantitative Proteomics

Cells were lysed in 7M urea, 2M thiourea, 4% CHAPS using sonification in Bioruptor. Proteins (20 µg) were digested using a modified filter-aided sample preparation (FASP) protocol(1) and the resulting tryptic peptides were adjusted to a concentration of 500 ng/µL using 0.1% formic acid and spiked with 25 fmol/µL of enolase 1 (*Saccharomyces cerevisiae*) tryptic digest standard (Waters Corporation). NanoLC-MS analysis of tryptic peptides was performed as described before using a nanoAcquity UPLC system (Waters Corporation) coupled to a Waters Synapt G2-S HDMS mass spectrometer (Waters Corporation) (1). In brief, peptides were separated using a HSS-T3 C18 1.8 µm, 75 µm x 250 mm reversed phase column using 0.1% formic acid in H_2O as mobile phase A and 0.1% formic acid in

acetonitrile as mobile phase B. Samples were loaded onto the column in direct injection mode and peptides separated using a gradient from 1% to 35% mobile phase B over 90 min. NanoESI-MS analysis of tryptic peptides was performed using ion mobility enhanced MS^E on the Waters Synapt G2-S system as detailed before (2). Rawdata processing and database search were performed using ProteinLynx Global SERVER (PLGS, version 3.02, Waters Corporation). For protein identification, data were searched against a custom compiled database containing UniProtKB/Swiss-Prot entries of the mouse reference proteome (UniProtKB release 2012_07, 20,231 entries). Sequence information for enolase 1 (*Saccharomyces cerevisia*e) as well as common contaminants (i.e. human keratins, porcine trypsin). The following criteria were applied for database search: (i) trypsin as digestion enzyme, (ii) up to two missed cleavages per peptide, (iii) a minimum peptide length of six amino acids, (iv) carbamidomethyl cysteine as fixed and (v) methionine oxidation as variable modification. The false discovery rate (FDR) for peptide and protein identification was assessed searching a reverse database and set to 0.01 for database search in PLGS. Subsequent label-free quantification analysis was performed using the ISOQuant software tool (1, 2) . All samples were analyzed in four technical replicates.

Microbiota analyses

Fresh stools were collected from colons of cohoused *vFlip*$^{IEC\text{-}tg}$ mice and littermate controls. Bacterial genomic DNA from stools was isolated using a QIAamp DNA Stool Mini Kit (Qiagen, Hilden, Germany) including a bead-beating step and quantified using a Qbit device (Thermofisher). The V3+4 region of the 16S rRNA gene was amplified using 10 ng of bacterial template DNA with degenerate region-specific primers containing barcodes and Illumina flow cell adaptor sequences (3) in a reaction consisting of 25 PCR cycles (98 °C 15 sec, 58 °C 20 sec, 72 °C 40 sec) using the NEBNext Ultra II Q5 Master Mix (New England Biolabs). Amplicons were purified with Agencourt AMPure XP Beads (Beckmann Coulter), normalized and pooled before sequencing on an Illumina miseq device using a 600-cycle paired-end kit and the standard Illumina HP10 and HP11 sequencing primers. Subsequently,

the read fastq files were bioinformatically processed (merging, demultiplexing, quality filtering, dereplication, chimera removal) using the 64 bit version of Usearch 10 according to the Uparse pipeline (4). Operational taxonomic units (OTUs) were picked at a threshold of 97 % similarity and taxonomically classified by comparing the representative OTU sequence to the reference file of the ribosomal database project (RDP version 16). Alpha diversities, samples distances and relative differential abundances after rarifying were calculated with Microbiomeanalysist (5).

Cultivation of eukaryotic cells

In this study, the Human colorectal adenocarcinoma cell line HT29 (ATCC®, HTB-38™) and iSLK.rHHV8.219 cells stably infected with rHHV8.219 virus (kindly provided by Don Ganem (6)) were used. iSLK cells were recently shown to be derived from the clear-cell renal-cell carcinoma cell line Caki-1 (7). HT29 and HT29.rHHV8.219 cells were cultured in McCoy's 5A + GlutaMax-I (Life Technologies) medium supplemented with 10 % FCS at 37 °C in a humidified atmosphere with 5 % CO_2. iSLK.rHHV8.219 cells were cultured in DMEM (Life Technologies) supplemented with 2 mM L-Glutamine (Life Technologies) and 10 % FCS (Biochrom) at 37 °C in a humidified atmosphere with 8.5 % CO_2. In addition, puromycin (1 µg/ml, Sigma-Aldrich) was freshly added to the rHHV8.219 infected cells in culture.

Lipofectamine transfection

Transfection of HT29 cells with expression plasmids (8) was performed using lipofectamine 2000 (Life technologies) following the manufacturer's protocol. Briefly, HT29 cells were seeded 24 h prior to transfection at a density of 3×10^5 cells per well of a six well plate. 10 µl lipofectamine was added to 250 µl OptiMEM (Life Technologies) and incubated for 10 min at RT. Subsequently, 5 µg DNA in 250 µl OptiMEM were added to a total volume of 500 µl. The transfection mixture (lipofectamine + DNA) was then added dropwise to cells cultivated with 1.5 ml full medium. After 4 h of incubation, cells were washed once with 1x PBS, then fresh medium was added and cells were further incubated until harvesting.

Flow cytometry

48 h and 72 h post transfection, the cell supernatant was collected in a tube and the cells were detached using PBS containing 1 mM EDTA (Sigma-Aldrich) and re-suspended in the cell supernatant. Then the tubes were centrifuged at 500 x g for 5 min. Afterwards, the cells were washed twice with FACS buffer (1x PBS + 1 mM EDTA + 2% FCS), centrifuged and re-suspended in FACS buffer with 0.4 µg/ml propidium iodide (Invitrogen). The cells were then incubated for 15 min at room temperature. Flow cytometry was performed using a FACSCalibur cytometer (BD Biosciences). For each condition, 10.000-30.000 cells were counted. Results were analyzed with the CellQuestPro software (BD Biosciences).

Virus production and infection of HT29 cells

iSLK.rHHV8.219 were treated with 1 µg/ml doxycycline (Life technology) to induce lytic replication. 96 h later, the supernatant was collected and debris was removed by centrifugation (500 x g; 5 min; 4 °C). Subsequently, the supernatant was first filtered (0.45 µm) and the cleared supernatant was further used for infection. Infection of cells was done by spinning the cleared supernatant on cells at 500 x g for 20 min at 32 °C in presence of polybrene (8 µg/ml, Sigma-Aldrich). Medium was changed on the following day. 48 h post-infection, cells were harvested for flow cytometry.

Supplementary Figure Legends

Suppl. Fig. 1: *vFlip* expression in IECs induces colitis *in vivo*.

(A) Representative pictures of GFP fluorescence staining of cross sections from different organs of indicated mice. Scale bar 50 µm. (B) Representative pictures of a *vFlip*$^{IEC\text{-}tg}$ and control mouse. (C) Analysis of body weight of control (n=12) and *vFlip*$^{IEC\text{-}tg}$ (n=9) mice at the age of 4 weeks, **p<0.01. (D) Representative endoscopic pictures and H&E staining from the colon of indicated mice. Scale bar middle panel 500 µm, right panel 100 µm. (E) Histology score of H&E stained colon cross sections of control (n=16) and *vFlip*$^{IEC\text{-}tg}$ (n=21) animals, ***p<0.001. (F) Transcriptional analysis of *Tnfa* (n≥10) and *S100a9* (n≥9) in the colon of control and *vFlip*$^{IEC\text{-}tg}$ mice. Values are shown +SD and were calculated relative to control mice. *Hprt* was used as internal standard. Data were pooled from 3 individual experiments, **p<0.01, ***p<0.001.

Suppl. Fig. 2: HHV8 infection of HT29 cells.

(A) Representative microscopic pictures of GFP fluorescence of HT29 cells uninfected or infected with GFP-fused rHHV8.219 for 48 h. Arrow points to infected cells. Scale bar 50 µm. (B) FACS analysis of GFP fluorescence in uninfected and rHHV8.219-infected HT29 cells 48 h post infection. Infection was performed in triplicates. (C) Western Blot analysis of RIP3 and MLKL in uninfected and rHHV8.219-infected HT29 cells 48 h post infection. GAPDH was used as loading control. (D) Densitometric analysis of RIP3 and MLKL protein levels normalized to GAPDH. UI = uninfected.

Suppl. Fig. 3: Cell death induction by *vFlip* expression *in vitro*.

HT29 cells were not transfected or transfected with indicated plasmids. 48 h and 72 h after transfection cells were harvested, stained with PI and analyzed by FACS. Transfection was performed in triplicates, ns =not significant, *p<0.05, **p<0.01, ***p<0.001.

Suppl. Fig. 4: vFLIP induced inflammation and Paneth cell loss is independent of RIP3.

Representative Colonoscopy pictures, H&E staining of small and large intestine (Scale bar 100 µm) and immunohistochemical lysozyme staining on small intestinal sections (Scale bar 75 µm) of indicated mice.

Suppl. Fig. 5: vFLIP induces changes in the microbial composition.

Fresh fecal samples were collected from colons of cohoused *vFlip*$^{IEC\text{-}tg}$ mice (n=5) and control littermates (n=7). (A) Alpha diversities (diversity within a given sample) in stools of *vFlip*$^{IEC\text{-}tg}$ and control mice were calculated based on the Shannon index, which accounts for both abundance and evenness of the species present. (B) Beta diversity analysis (inter-individual variability of microbial communities) was analyzed by principle coordinate analysis (PcoA) at species level using Bray-Curtis dissimilarity. Points that are closer together on the ordination have communities that are more similar. Ellipses were drawn using a confidence interval of 95% for each group. (C) Relative abundances of *Proteobacteria* in *vFlip*$^{IEC\text{-}tg}$ and control mice. (D) Heat map illustration of relative abundances of selected bacterial genera.

Suppl. Fig. 6: Paneth cell loss and colitis in *vFlip*$^{IEC\text{-}tg}$ mice is dependent on *Ikka*.

(A) Western Blot analysis of IKKα, IKKβ and GFP using IEC lysates of indicated mice. Actin was used as a loading control. (B) Western Blot analysis of lysozyme using IEC lysates of indicated mice. Actin was used as a loading control. (C) Representative endoscopic pictures and H&E staining from the colon of indicated mice. Scale bar 100 µm.

References

1. Distler U, Kuharev J, Navarro P, Tenzer S. Label-free quantification in ion mobility-enhanced data-independent acquisition proteomics. Nature protocols. 2016;11(4):795-812.
2. Distler U, Kuharev J, Navarro P, Levin Y, Schild H, Tenzer S. Drift time-specific collision energies enable deep-coverage data-independent acquisition proteomics. Nature methods. 2014;11(2):167-70.
3. Fadrosh DW, Ma B, Gajer P, Sengamalay N, Ott S, Brotman RM, et al. An improved dual-indexing approach for multiplexed 16S rRNA gene sequencing on the Illumina MiSeq platform. Microbiome. 2014;2(1):6.
4. Edgar RC. UPARSE: highly accurate OTU sequences from microbial amplicon reads. Nature methods. 2013;10(10):996-8.
5. Dhariwal A, Chong J, Habib S, King IL, Agellon LB, Xia J. MicrobiomeAnalyst: a web-based tool for comprehensive statistical, visual and meta-analysis of microbiome data. Nucleic acids research. 2017;45(W1):W180-W8.
6. Myoung J, Ganem D. Generation of a doxycycline-inducible KSHV producer cell line of endothelial origin: maintenance of tight latency with efficient reactivation upon induction. Journal of virological methods. 2011;174(1-2):12-21.
7. Sturzl M, Gaus D, Dirks WG, Ganem D, Jochmann R. Kaposi's sarcoma-derived cell line SLK is not of endothelial origin, but is a contaminant from a known renal carcinoma cell line. International journal of cancer. 2013;132(8):1954-8.
8. Sander G, Konrad A, Thurau M, Wies E, Leubert R, Kremmer E, et al. Intracellular localization map of human herpesvirus 8 proteins. Journal of virology. 2008;82(4):1908-22.